PERGAMON

International Journal of Heat and Mass Transfer 45 (2002) 3429–3436

International Journal of HEAT and MASS TRANSFER

www.elsevier.com/locate/ijhmt

Bed-to-wall heat transfer behavior in a pressurized circulating fluidized bed

A.V.S.S.K.S. Gupta, P.K. Nag *

Department of Mechanical Engineering, Indian Institute of Technology, Kharagpur 721 302, India

Received 23 April 1998; received in revised form 23 November 2001

Abstract

An experimental investigation has been made to study the effect of pressure and other relevant operating parameters on bed hydrodynamics and bed-to-wall heat transfer in a pressurized circulating fluidized bed (PCFB) riser column of 37.5 mm internal diameter and 1940 mm height. The experiments have been conducted with and without bed material for the consideration of frictional pressure drop due to gas density at elevated pressures. The pressure drop measured without sand particles is assumed as the pressure drop due to gas density for the calculation of bed voidage and suspension density profiles. The specially designed heat transfer probe is used to measure the bed-to-wall heat transfer coefficient. The experimental results have been compared with the published literature and good agreement has been observed. The axial bed voidage is less in the bottom zone of the riser column and is increasing along the height of the bed. With the increase in system pressure, the bed voidage is found to be increasing in the bottom zone and decreasing in the top zone. The heat transfer coefficient increases with the increase in system pressure as well as with the gas superficial velocity. The heat transfer coefficient is also observed to be increasing with the increase in average suspension density. © 2002 Published by Elsevier Science Ltd.

1. Introduction

The pressurized circulating fluidized bed (PCFB) combustion technology is outstanding in its fuel flexibility, compact furnace size, environmental compatibility, efficient combustion and good heat transfer characteristics, and therefore, it has become a subject of worldwide attention as a new technique for coal fired steam generation as well as for combined cycle power generation. This technology-applied boilers are still at testing level and a few pilot plants have been installed in the world so far. The results from these pilot plants are encouraging and forecasting PCFB as a promising technology which is likely to be used for future power plants with coal-based combined cycle. The design of such a boiler is largely based on knowledge of bed hydrodynamics and heat transfer.

At atmospheric condition, the bed hydrodynamics and heat transfer have been reviewed by many investigators [1–5]. The effect of pressure and temperature on fluidized beds is critically reviewed by Yates [6]. The cminimum fluidization velocity, the bubbling velocity and the terminal velocity were found to be decreasing with the increase of operating pressure. But very few published papers are available on hydrodynamics and heat transfer in a CFB operated at elevated pressures. Plasynski et al. [7] studied the variation of the pressure gradient in a 26 mm diameter tube with glass beads and coal as the bed material and nitrogen as the fluidizing gas for different operating pressures. Reddy and Knowlton [8] also investigated the effect of operating pressure on CFB riser hydrodynamics in a 300 mm diameter tube and obtained results exactly contradictory to those obtained by Plasynski et al. [7]. The difference between the results obtained by them is due to higher gas pressure drop in the smaller tube compared to that in the larger diameter tube. Tsukada et al. [9] reported the effect of pressure on transport velocity in a CFB and observed that the core diameter at transport velocity is

* Corresponding author. Tel.: +91-3222-55221; fax: +91-3222-55303.

E-mail address: pknag@mech.iitkgp.ernet.in (P.K. Nag).

0017-9310/02/$ - see front matter © 2002 Published by Elsevier Science Ltd.
PII: S0017-9310(01)00365-9

Nomenclature

d_p	average diameter of sand particles, μm	Q	heat transfer rate, W
g	acceleration due to gravity, m/s^2	T_b	bed temperature, °C
H	distance between the two pressure tappings, m	T_w	wall temperature, °C
		u	gas superficial velocity, m/s
h	bed-to-wall heat transfer coefficient, W/m^2 K	Δp	measured pressure drop, mm of H_2O
I	bed inventory, kg	ρ_s	bulk density of the sand, kg/m^3
K	thermal conductivity of inconel, W/m K	ρ_g	density of gas, kg/m^3
L	height of the heat transfer probe, m	ρ_{sus}	average suspension density, kg/m^3
p	operating pressure, bar	ε	bed voidage

80% of the bed diameter and the thickness of the annulus is slightly decreasing with the operating pressure.

Shen et al. [14] investigated the bed-to-wall heat transfer in a CFB at high pressures. Wirth [15,16] and Molerus [17,18] carried out some experiments in a PCFB and the results were presented in terms of dimensionless numbers. After observing the published literature there is still large dearth of information regarding the bed hydrodynamics and the heat transfer in a CFB at elevated pressures. In the present investigation an attempt has been made to furnish more experimental data in this regard.

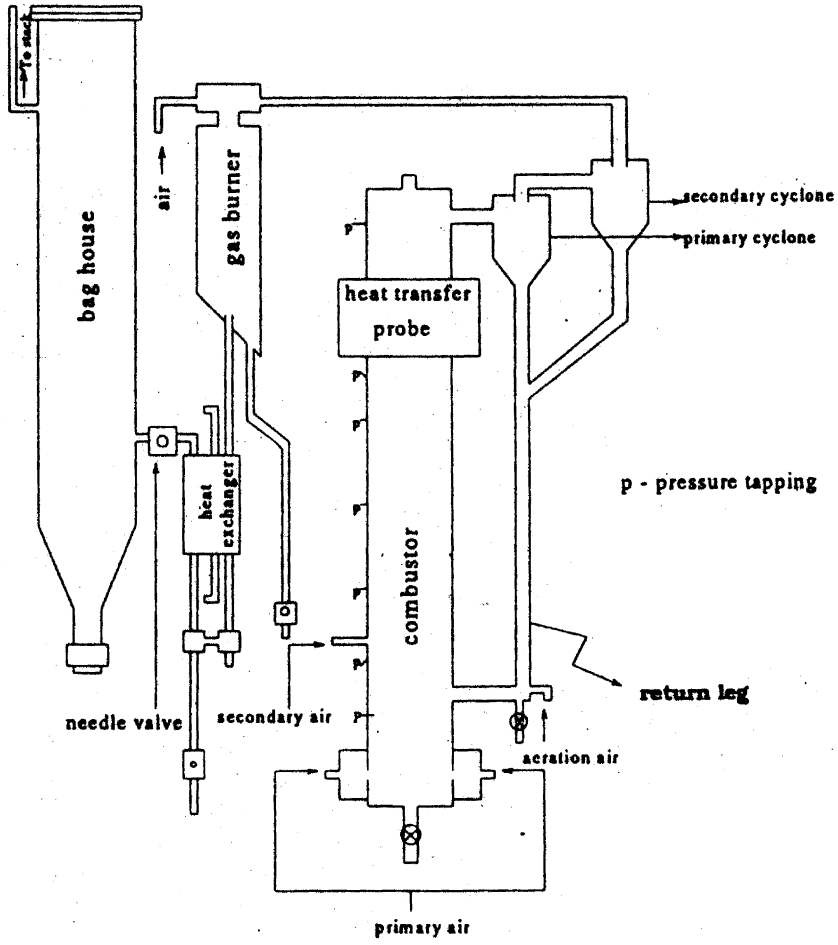

Fig. 1. Schematic diagram of the experimental setup (PCFB).

2. Experimental setup

A schematic diagram of the experimental setup is shown in Fig. 1. The PCFB riser column is made of inconel, of 37.5 mm internal diameter and 1940 mm height. The compressed air is passed through a filter first to remove the traces of moisture and oil before it is drawn into a common manifold. The manifold branches into a number of air supply lines amongst which three lines go to the riser column viz., primary air, secondary air and L valve air (aeration air). Each of the air lines is provided with a set of a control valve and a rotameter. The primary air enters through an annular ring on the side wall of the column. The diameter of the column being small, the quality of the fluidization is not affected substantially due to the side entrance of the primary air. On the other hand, the absence of the distributor plate allows an unrestricted path of quick drainage of the entire bed material from the column. The riser is connected with two cyclones in series, both of which are joined to a single return leg. One L-valve is provided at the bottom of this common return leg to supply the aeration air so as to maintain the re-circulation of the bed material.

Seven pressure tappings are provided at different heights of the riser column to measure the pressure drops. Cigarette filters are used at the pressure tapping ends to minimize the pressure fluctuations and to avoid the escape of sand particles from the column. Pressure drops are measured with a differential pressure transducer which is calibrated and compared with the calibration curve supplied by the manufacturer. Each air line is provided with a separate flow control valve and a rotameter to control and to measure the air flow rate. All the rotameters, the flow control valves and the differential pressure transducer are fixed to a single control panel board.

The heat transfer probe is located at a height of 1500 mm above the primary air entrance level of the riser column. The internal diameter, outer diameter and height of the heat transfer probe are 37.5, 100 and 100 mm, respectively. Nine thermocouples are embedded into the heat transfer probe at three different radial and axial locations (Fig. 2) to measure the radial and the axial temperature variations in the heat transfer probe. Two thermocouples, one above the heat transfer probe and the other below it are provided to measure the bed temperatures. Another thermocouple is provided in the wall to measure the wall temperature. Chromel–alumel thermocouples are used to measure all these temperatures. The riser column, the return leg and the cyclones are housed in an electrically heated and properly

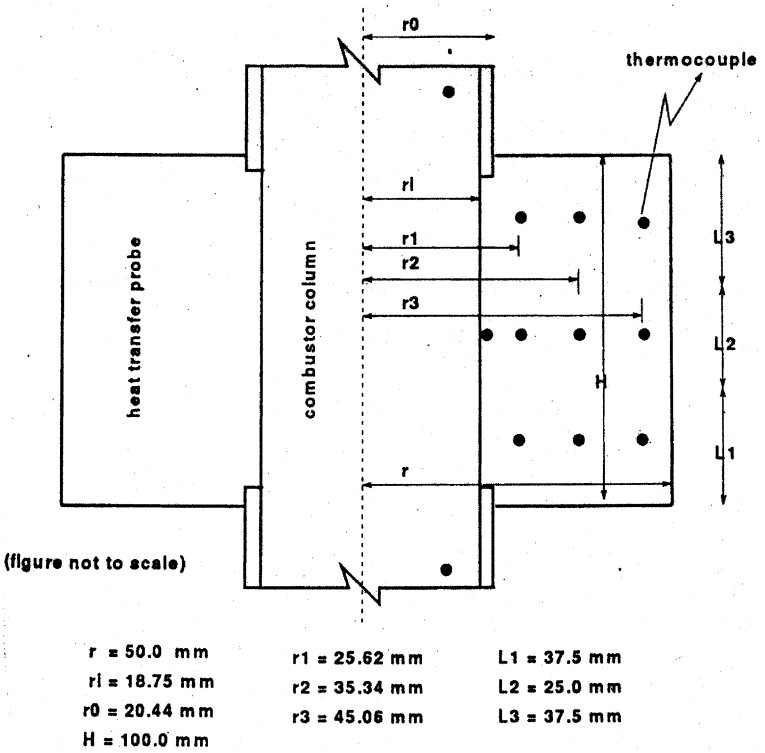

Fig. 2. Schematic diagram of the heat transfer probe.

insulated chamber. 10 plate heaters of rating 1350 W each are located in different zones of the chamber for uniform heating throughout the bed so as to avoid differential thermal expansion in various regions of the setup. A controller which acts as a thermostat is provided to maintain the desired chamber temperature.

Experiments have been carried out for different pressures ranging from 2 to 6 bar for different velocities ranging from 0.25 to 1.25 m/s, for different bed inventories 1.00, 1.25 and 1.50 kg and for different furnace temperatures 400, 450 and 500 °C. Local sand of average particle size 264 μm is used as the bed material. Operating pressure and primary velocity are controlled using pressure regulator, flow control valve and needle valve located between the heat exchanger and the bag filter. The amount of aeration air is negligible compared to the primary air, and the air velocity is not substantially affected by the aeration air.

3. Results and discussion

As explained by Reddy and Knowlton [8], the pressure drop due to gas density is inversely proportional to the diameter raised to the power of 1.25. In the present experiments, the diameter of the tube is small and this pressure drop is high. The measured pressure drop across the test section consists of the frictional pressure drop due to gas density and the weight of the bed. To consider the frictional pressure drop, the experiments have been conducted with and without sand particles. The pressure drop measured without sand particles is assumed as the frictional pressure drop and it is subtracted from the pressure drop measured with sand particles for calculating the voidage profiles and the average suspension density.

The bed voidage is calculated by

$$\text{Voidage}(\varepsilon) = 1 - \frac{\Delta p}{\rho_s g H}, \tag{1}$$

where (Δp) is the pressure drop difference with and without sand particles.

The average cross-sectional suspension density is calculated by

$$\text{Average suspension density}(\rho_{sus}) = (1-\varepsilon)\rho_s + \varepsilon\rho_g, \tag{2}$$

where ρ_g is the gas density and it is estimated for different pressures by assuming the ideal gas equation.

The bed-to-wall heat transfer coefficient is estimated from the measured bed temperature, wall temperature and the temperatures in the heat transfer probe by energy balance between bed-to-wall convection and conduction heat transfer in the probe.

Bed-to-wall heat transfer due to convection is given as

$$Q = 2\pi r_1 L h[T_b - T_w]. \tag{3}$$

Heat transfer in the heat transfer probe is given as

$$Q_k = \frac{2\pi K L(T_w - T_k)}{\ln(r_1/r_2)}, \tag{4}$$

$$T_k = \frac{T_{k1} + T_{k2} + T_{k3}}{3}, \tag{5}$$

$$Q = \frac{Q_1 + Q_2 + Q_3}{3}. \tag{6}$$

The bed-to-wall heat transfer coefficient is found out by equating Eqs. (3) and (6).

Fig. 3 shows the variation of average cross-sectional bed voidage along the height of the bed for a given velocity and for different operating pressures. It is observed that the bed voidage is low in the bottom region of the bed and it is high in the top region. As the pressure increases, the bed voidage is increasing in the bottom region and decreasing in the top region. At low pressures the solids are concentrated at the bottom region and the drag force is less on the solid particles, resulting in less voidage. With increase in the pressure, the carryover of the solid particles from the lower region of the bed increased due to increase in drag force which results in increased particle concentration at the top region.

Fig. 4 depicts the variation of average cross-sectional bed voidage along the height of the bed for different gas superficial velocities for a particular pressure. It is found that the bed voidage is low at the bottom section for the lower velocity and increases towards the riser exit. At lower gas superficial velocity, the solid concentration is maximum at the bottom region and it increases with the

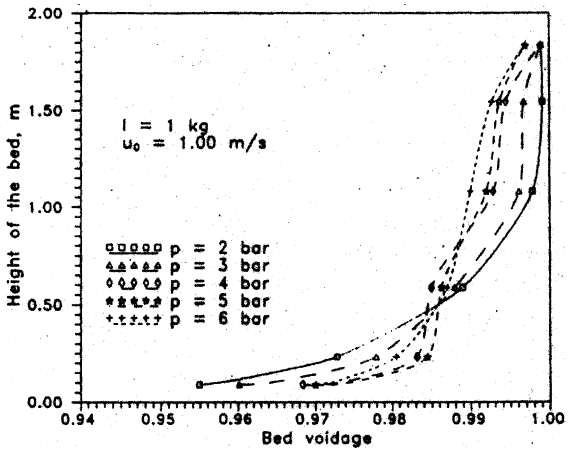

Fig. 3. Effect of operating pressure on bed voidage along the height ($I = 1.0$ kg, $u_0 = 1.00$ m/s).

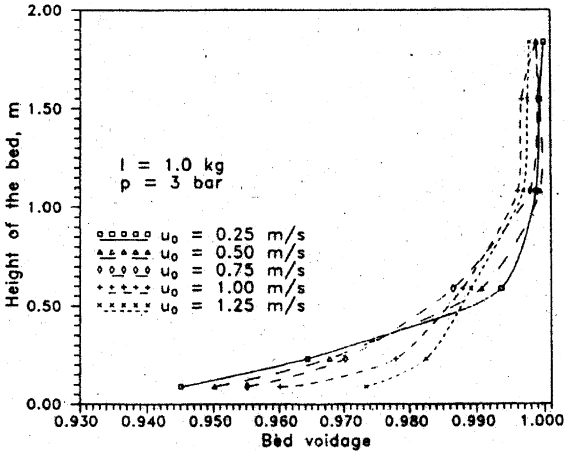

Fig. 4. Effect of gas superficial velocity on bed voidage along the height ($I = 1.0$ kg, $p = 3$ bar).

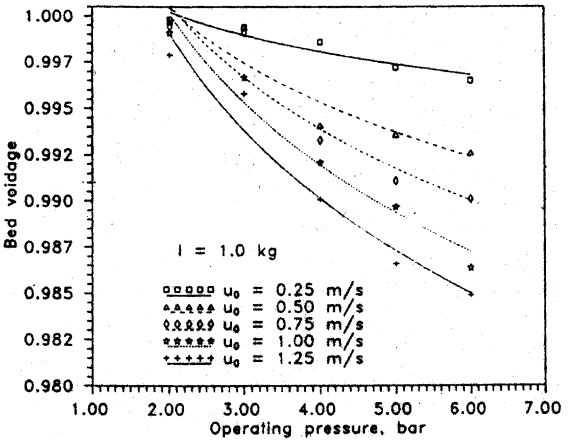

Fig. 6. Effect of operating pressure on bed voidage at the height of 1545 mm above the primary air level ($I = 1.0$ kg).

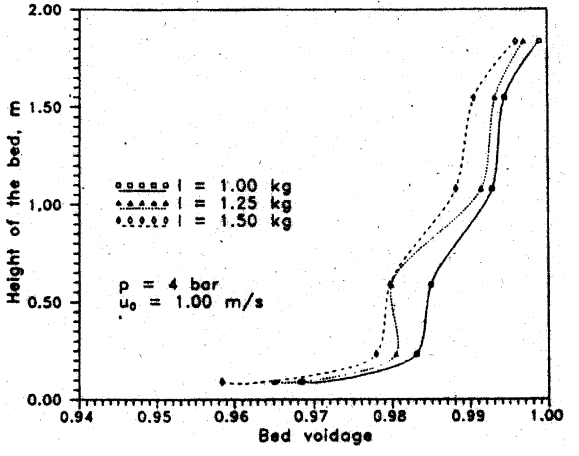

Fig. 5. Effect of bed inventory on bed voidage along the height ($p = 4$ bar, $u_0 = 1.00$ m/s).

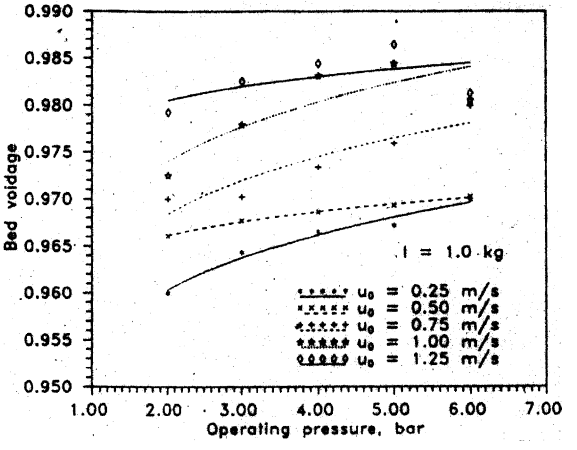

Fig. 7. Effect of operating pressure on bed voidage at the height of 232.5 mm above the primary air level ($I = 1.0$ kg).

increase in gas superficial velocity. With the rise in primary air velocity, more solids are lifted up due to more drag force resulting in the increase in bed voidage in the bottom portion and decrease in the top region.

The effect of bed inventory on bed voidage profile along the riser height for a specific pressure and for a particular velocity is shown in Fig. 5. It is to be noted that the bed voidage along the height of the bed is decreasing with the increase in bed inventory. The concentration of sand particles is more in the riser column for the higher bed inventory and hence, the bed voidage.

The variation of bed voidage at the height of 1545 mm above the primary level with the operating pressure is shown in Fig. 6. The bed voidage is found to be decreasing with increase in operating pressure and also with gas superficial velocity. At 232.5 mm above the primary air level, the bed voidage is found to be decreasing with the system pressure which is shown in Fig. 7. At high pressure, more drag force is acting on the bed material in the bottom zone with the bed material being lifted to the top zone, which results in less voidage at the top zone.

Figs. 8–10 show the variation of the average suspension density along the height of the bed for different values of pressures, for different values of gas superficial velocities and for different bed inventories. The average suspension density profile along the height of the bed shows two different zones, viz., a dense phase bottom zone and a dilute phase top zone. The suspension

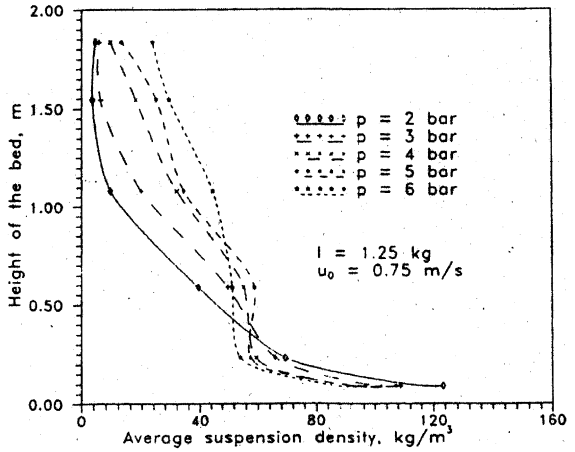

Fig. 8. Effect of operating pressure on average suspension density along the height of the bed ($I = 1.25$ kg, $u_0 = 0.75$ m/s).

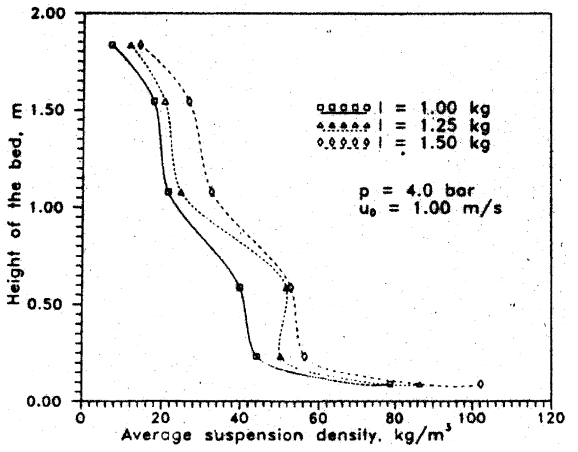

Fig. 10. Effect of bed inventory on average suspension density along the height of the bed ($p = 4$ bar, $u_0 = 1.00$ m/s).

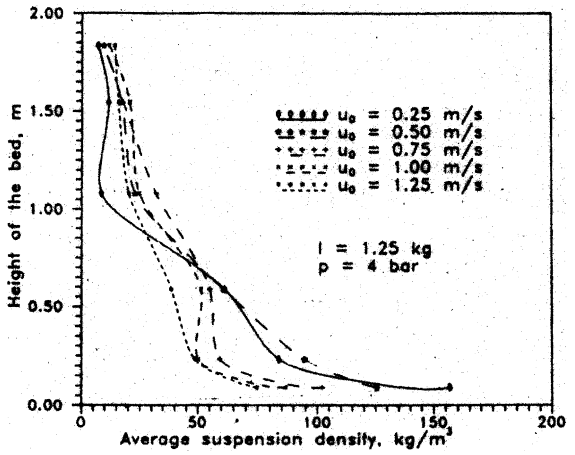

Fig. 9. Effect of gas superficial velocity on average suspension density along the height of the bed ($I = 1.25$ kg, $p = 4$ bar).

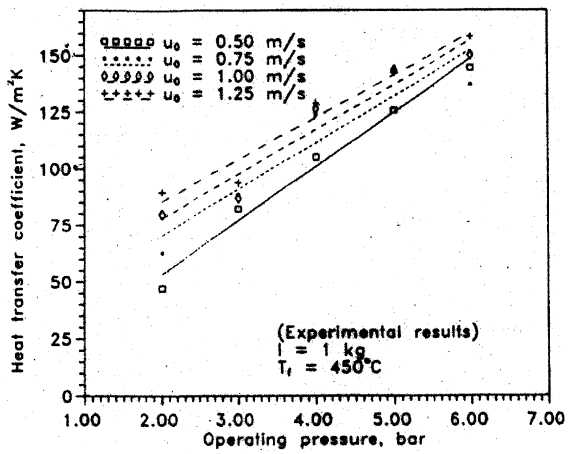

Fig. 11. Effect of operating pressure on heat transfer coefficient for different gas superficial velocities ($I = 1.0$ kg, $T_f = 450$ °C).

density in the bottom zone is decreasing and is increasing in the top zone with the increase in the operating pressure. With the increase in gas superficial velocity, the suspension density decreases in the bottom zone and increases in the top zone, so that the bed is becoming uniform along the height of the bed. An increase in bed inventory also improves the suspension density at all sections in the riser column.

Fig. 11 shows the effect of pressure on bed-to-wall heat transfer coefficient for different velocities. It is found that the heat transfer coefficient increases monotonically with increase in the operating pressure as well as with the increase in gas superficial velocity. At elevated pressure, the gas phase convective heat transfer is more due to high density of gas. This enhances the heat transfer rate and hence, the heat transfer coefficient.

Fig. 12 demonstrates the variation of heat transfer coefficient with gas superficial velocity for different pressures. It is observed that the heat transfer coefficient increases with the increase in velocity. This may be due to enhanced turbulence at higher velocity which in turn causes intermixing between the solids and gas–solid suspension. Hence, high heat transfer coefficient ensues at higher velocities.

Figs. 13 and 14 depict the change in heat transfer coefficient with varying average suspension density as observed with the earlier works [10,11,13,17]. It is noticed that the heat transfer coefficient increases with the increasing cross-sectional average suspension density.

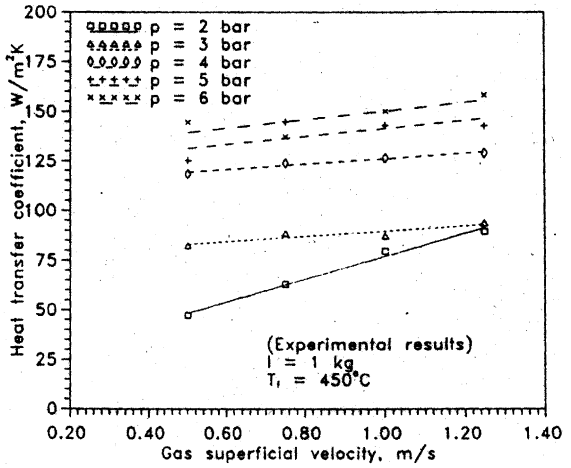

Fig. 12. Effect of gas superficial velocity on heat transfer coefficient for different operating pressure ($I = 1.00$ kg, $T_f = 450$ °C).

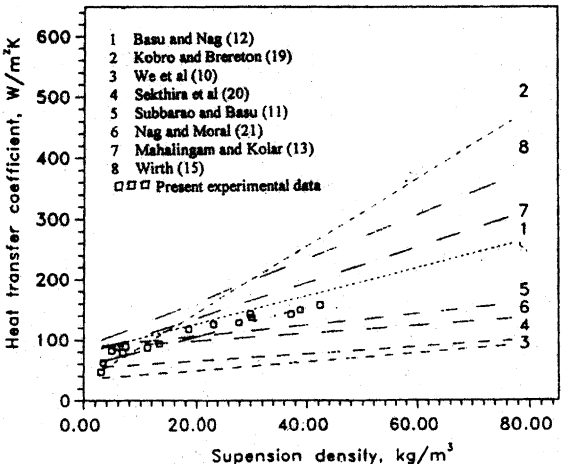

Fig. 14. Comparison of present results with published literature [10–13,15,19–21].

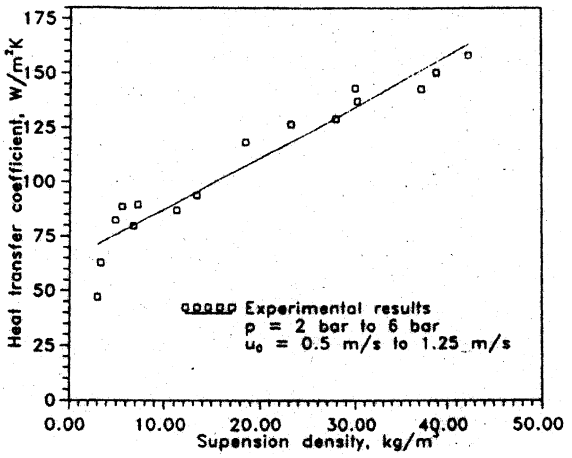

Fig. 13. Effect of suspension density on heat transfer coefficient in a PCFB (experimental results).

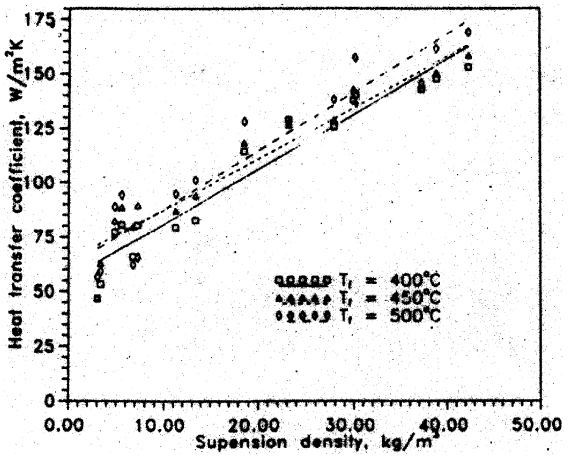

Fig. 15. Effect of furnace temperature on heat transfer coefficient.

This is as expected because thermal capacity of solids is much higher for higher values of average suspension density. Inspite of different operating conditions and different operating equipment being used in these studies, the present data with the suspension density is fairly comparable with published results. The effect of bed temperature on heat transfer coefficient in the PCFB riser is shown in Fig. 15, which shows heat transfer coefficient increasing with the bed temperature. This may be due to higher thermal conductivity of gas and higher radiative component at higher temperatures. Fig. 16 shows the variation of local heat transfer coefficient along the height of the probe for different pressures. The local heat transfer coefficient significantly increases with the increase in pressure and not much with the increasing height.

4. Conclusion

The axial bed voidage along the height of the bed is observed to be less in the bottom zone and is high in the top zone. It is also observed that the bed voidage increases in the bottom zone and decreases in the top zone with increase in operating pressure. The heat transfer coefficient is found to be increasing with the increase in operating pressure as well as increase in gas superficial velocity. It also increases monotonically with increasing

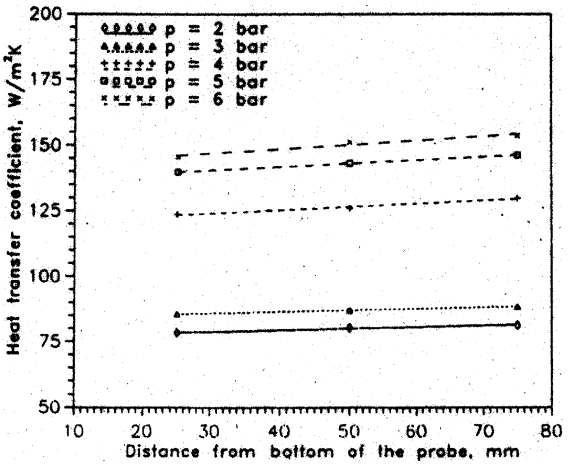

Fig. 16. Variation of local heat transfer coefficient along the height of the heat transfer probe.

bed temperature. The data show trends similar to those in published literature.

References

[1] F. Berruti, J. Chauoki, L. Godfroy, T.S. Pugsley, G.S. Patience, Hydrodynamics of circulating fluidized bed risers: a review, Can. J. Chem. Eng. 73 (1995) 579–602.

[2] J.R. Grace, Heat transfer in circulating fluidized beds, in: P. Basu (Ed.), Circulating Fluidized Bed Technology, Pergamon, Canada, 1986, pp. 63–81.

[3] L.R. Glicksman, Circulating fluidized bed heat transfer, in: P. Basu, J.F. Large (Eds.), Circulating Fluidized Bed Technology, vol. II, Pergamon, Oxford, 1988, pp. 13–29.

[4] B. Leckner, Heat transfer in circulating fluidized beds, in: P. Basu, M. Hasatani, M. Hario (Eds.), Circulating Fluidized Bed Technology, vol. III, Pergamon, Oxford, 1991, pp. 27–38.

[5] P. Basu, P.K. Nag, Heat transfer to walls of a circulating fluidized bed furnace, Chem. Eng. Sci. 51 (1996) 1–26.

[6] J.G. Yates, Effects of temperature and pressure on gas solid fluidization, Chem. Eng. Sci. 51 (1996) 167–205.

[7] S. Plasynski, G. Klinzing, M. Mathur, High pressure vertical pneumatic transport investigation, Powder Technol. 79 (1994) 95–109.

[8] S.B.K. Reddy, T.M. Knowlton, The effect of pressure on CFB riser hydrodynamics, Proceedings of the 5th International Conference on CFB, Beijing, DB15 (CFB V preprints), 1996.

[9] M. Tsukada, D. Nakanishi, M. Horio, Effect of pressure on transport velocity in a circulating fluidized bed, in: 4th International Conference on CFB, Pennsylvania (preprint volume), 1994, pp. 248–253.

[10] R.L. Wu, J.R. Grace, C. Jim, C.M.H. Brereton, Suspension to wall heat transfer in a circulating fluidized bed combustor, AIChE J. 35 (1989) 1685–1691.

[11] D. Subbarao, P. Basu, A model for heat transfer in circulating fluidized beds, Int. J. Heat Mass Transfer 29 (1986) 487–489.

[12] P. Basu, P.K. Nag, An investigation into heat transfer in circulating fluidized bed, Int. J. Heat Mass Transfer 30 (1987) 2399–2409.

[13] M. Mahalingam, A.K. Kolar, Emulsion layer model for wall heat transfer in a circulating fluidized bed, Chem. Eng. Sci. 37 (1991) 1139–1150.

[14] X. Shen, N. Zhou, Y. Xu, Experimental study on heat transfer in a pressurised circulating fluidized bed, in: P. Basu, M. Hasatani, M. Hario (Eds.), Circulating Fluidized Bed Technology, vol. III, Pergamon, New York, 1991, pp. 451–456.

[15] K.E. Wirth, Heat transfer in circulating fluidized beds, Chem. Eng. Sci. 50 (1995) 2137–2151.

[16] K.E. Wirth, Prediction of heat transfer in circulating fluidized beds, in: 4th International Conference on Circulating Fluidized Beds, Pennsylvania (preprint volume), 1994, pp. 344–349.

[17] O. Molerus, Arguments on heat transfer in gas fluidized beds, Chem. Eng. Sci. 48 (1993) 761–770.

[18] O. Molerus, Fluid dynamics and its relevance for basic features of heat transfer in circulating fluidized beds, in: 4th International Conference on Circulating Fluidized Beds, Pennsylvania (preprint volume), 1994, pp. 338–343.

[19] H. Kobro, C. Brereton, Control and fuel flexibility of circulating fluidized beds, in: P. Basu (Ed.), Circulating Fluidized Bed Technology, Pergamon, New York, 1986, pp. 263–273.

[20] A. Sekthira, Y.Y. Lee, G.E. Genetti, Heat transfer in circulating fluidized beds, in: Proceedings of the 25th National Heat Transfer Conference, Houston, Texas, 1988, pp. 24–27.

[21] P.K. Nag, M.N. Ali Moral, Effect of probe size on heat transfer at the wall in circulating fluidized beds, Int. J. Energy Res. 14 (1990) 965–974.